Advancements on Real-Time Simulation for High Switching Frequency Power Electronics Applications

(Invited Paper)

Caio R. D. Osório, Milos Miletic, Jovan Zelic, Dusan Majstorovic, Ognjen Gagrica
Typhoon HIL, Inc.
Novi Sad, Serbia
Email: (caio.osorio, milos.miletic, jovan.zelic, dusan, ognjen.gagrica)@typhoon-hil.com

***Abstract*—This paper presents an outlook about controller hardware-in-the-loop technology and how recent advancements in time resolution improved real-time simulation accuracy for testing high switching frequency power electronics applications. To illustrate that, the control of a dual active bridge converter (DAB) is taken as an example. The DAB converter is emulated on Typhoon HIL device, while the control algorithm is implemented on a digital signal processor from Texas Instruments. Real-time simulations are performed, highlighting the increased precision of the results obtained with the novel switch-level gate-drive signal oversampling.**

***Index Terms*—controller hardware-in-the-loop, dual active bridge, time resolution, power electronics, real-time simulation.**

I. Introduction

One of the key features that enabled the paradigm shift from centralized generation to distributed generation based on renewable energy sources was the accelerated development and continuous advancements on power electronics (PE) technology, allowing to achieve rapid cost reduction as well as increased reliability and improved power quality [1]. As a consequence, engineers are continuously challenged to design and implement different solutions more and more efficiently, which calls for different tools and can be specially demanding considering the need to comply with different requirements, such as grid codes and electric vehicle (EV) integration standards [2], [3]. In this direction, the strategy of waiting until late stages of a project to verify the integration of different hardware and software, as well as to assess the performance of the systems against test protocols, is no longer suitable. Even if scaled prototypes are considered, building the infrastructure can be time-consuming and expensive, and the test flexibility would still be limited by hardware constraints and also by the need to establish proper instrumentation and safety precautions [4]–[6].

For these reasons, the use of hardware-in-the-loop (HIL) for development and testing is an important alternative. This approach adds flexibility and security, besides reducing the time spent in different parts of the development cycle. Ergo, it has been a standard procedure in the automotive industry for more than two decades and it has also been recognized as a viable and cost-effective method for testing and pre-commissioning of microgrids [7], [8].

Considering PE industry, Controller-HIL (C-HIL) is an usual approach, where the power part can be simulated in real time, while the control and management systems, as well as the protection devices, can be implemented in the exact same platforms that will be embedded in the real apparatus. In this way, it possible to have a safe and high fidelity testing environment, where advanced control strategies and the interactions between different systems can be rapidly assessed without risking to damage the devices, reducing time and cost, besides improving test coverage and reproducibility [8], [9]. On the other hand, PE applications may encompass various switches operating at very high switching frequencies, especially considering the increasing use of wide bandgap devices in sectors such as the e-mobility industry. As a result, in order to capture the effects caused by the switching behavior, one has dynamically complex electrical systems that are really demanding to simulate with high fidelity in real time, requiring high resolution sampling of the gate drive signals (GDS) and very short simulation time steps and, therefore, advanced processing capability and ultralow latency [10], [11].

In this direction, this paper shows how C-HIL technology advanced, improving time resolution and therefore real-time simulation accuracy for high switching frequency applications. First, challenges related to the GDS sampling resolution are discussed and the Global GDS Oversampling method is introduced. A Boost converter operating at 80 kHz is used to illustrate the improvements on the accuracy as a result of this approach. Then, the Switch-level Oversampling method is presented, which allows to deal with more demanding high-switching frequency applications. To illustrate that, a dual active bridge (DAB) converter operating at 250 kHz is taken as a case study. The converter is emulated on the Typhoon HIL404 device, which is built for advanced motor drive and automotive applications, being able to reach simulation steps down to 200 ns with input sampling resolution of 3.5 ns. The control algorithm is implemented in the digital signal processor (DSP) TMS320F28379D, from Texas Instruments. Real-time simulations are performed and the accuracy of the obtained results is analyzed.

978-1-6654-0187-6/21/$31.00 ©2021 IEEE

II. Real-time Simulation for PE

Power electronics plants can be modeled based on ideal switches, neglecting dynamics associated to the transitions between switching states. Therefore, the semiconductors are either conducting or blocked, and the commutation between these two states is ideally fast. Nevertheless, real-time simulation devices run in discrete time and typically employ linear state-space equation solvers with fixed time step. To take into account the switching nature of the PE converters, a piece-wise linear approach can be used. In this scenario, the simulation dynamically changes among a finite number of modes, which are linear time-invariant models defined based on the possible states of the semiconductors (i.e., the reachable submodel topologies). Therefore, one has a fixed state-space representation over each simulation time step, for which the matrices can be computed offline during the compilation process and then stored in the solver memory [10].

On the other hand, note that the number of modes grows exponentially with the number of switches, which can lead to high memory resource requirements. To mitigate that, PE converters can be organized as pre-packaged components optimized for real-time execution, with an specialized run time logic that allows to reduce number of reachable modes. In addition, FPGA-based multi-core processors can be used, taking advantage of parallel computing to not only reduce the memory requirements but also to reduce the simulation step size. Those strategies are employed in the Typhoon HIL devices, as the ones used to obtain the results that will be presented in this paper.

As mentioned in the introduction, PE encompass a number of applications which require high-power converters that are operated at high frequencies, demanding high time resolution to achieve accurate simulation results. In this direction, considering fixed time step solvers, if the digital inputs are sampled only at the beginning of each simulation step, the sampling period of the pulse-width modulation signals is equal to the simulation time step. In addition, considering C-HIL applications, the simulation clock is not synchronized with the outputs of the connected digital controller. Therefore, since switching events can only be detected in the simulation step after the event has occurred, there is an inaccuracy to identify the exact instant where the digital input changed its state, leading to variable delays that cause imprecise duty cycle detection and hence inaccurate simulation results. The resulting sampling error depends on when the GDS changes with respect to the simulation steps, and the latency will be in the range from one to two simulation steps. This is shown in Figure 1, where DI represents the digital input (GDS) and X illustrates the state change due to the input event.

Ideally, in offline simulations, these outcomes could be mitigated by arbitrarily reducing the simulation time step at the expense of longer execution times, which is not viable for real-time simulators [13]. Thus, even FPGA based simulators are limited to simulation time steps of hundreds nano seconds, which still poses limitations to the accuracy of simulations for high switching frequency converters.

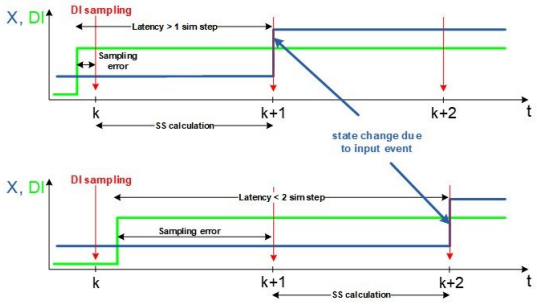

Fig. 1. Sampling error without GDS Oversampling [12].

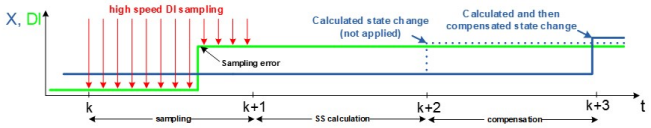

Fig. 2. Illustrative representation of the GDS Global Oversampling [12].

In this regard, although being able to reduce the simulation time step is important, additional strategies to enhance sampled GDS time resolution are also key features, as will be detailed in the next section [14].

III. Strategies for Time Resolution Enhancement

In the following subsections, two strategies for time resolution enhancement will be discussed, namely, the Global GDS Oversampling and the Switch-level GDS Oversampling.

A. Global GDS Oversampling

As mentioned before, the larger the simulation time steps, the larger the GDS sampling error can be, which will translate to larger errors in the state variables calculation. In order to meet high accuracy requirements with limited simulation step sizes, time resolution can be improved by using the Global GDS Oversampling method. In this approach, the driving signals are sampled multiple times within one simulation step, which allows to attenuate the sampling errors. Also, the switching events are time stamped, i.e, the time of the GDS transition is precisely captured, and then used to compensate the state variables [13], [15]. Figure 2 illustrates the Global GDS Oversampling method.

The Global GDS Oversampling algorithm can be summarized by the following steps [12]:

1. Sampling the GDS multiple times within a simulation step and identifying the instant when the change in the digital input occurs.
2. Calculation of the state variables without updating the GDS input. Meanwhile, information about the time when the GDS actually changed is used to calculate the value of states that will be used for the compensation in the next simulation step. These values are not visible at the outputs.

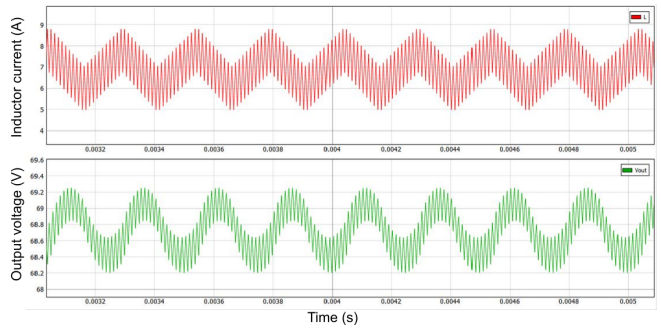

Fig. 3. Boost converter operating at 80 kHz: input current and output voltage without GDS oversampling.

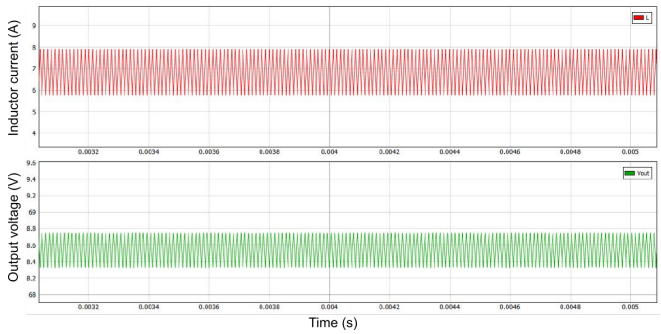

Fig. 4. Boost converter operating at 80 kHz: input current and output voltage with Global GDS oversampling enabled.

3. Third phase is the compensation of states. The temporary calculated states from the previously simulated step and information about the time when GDS changed are used to calculate new state output. After calculation and compensation, the correct value of the state will be present at the output.

To illustrate the improvements on simulation accuracy obtained with the Global GDS Oversampling method, let us consider a Boost converter operating in open-loop with a fixed duty cycle. The converter is driven by an external controller with switching frequency set to 80 kHz, while the real-time simulation runs on a Typhoon HIL402, with time step of 500 ns and GDS sampling period of 6.25 ns. Open-loop operation is chosen to emphasize the effects of the oversampling method without including controller dynamics in the comparison. Figure 3 shows the input current and the output voltage of the converter operating without GDS oversampling. In these results, we can see that the insufficient sampling resolution of the driving signal led to low frequency fluctuations on the converter states, which is an undesired behavior. On the other hand, when the Global GDS Oversampling feature is enabled, one has the results shown in Figure 4. Clearly, we can see that the low frequency fluctuations are mitigated, leading to the expected steady state behaviors.

As shown in the previous results, the Global GDS Oversampling method can significantly improve effective time resolution and therefore extend the range of switching frequencies that can be supported with high accuracy. However, this method leads to an increase in the computational burden and also to the need for an additional time step dedicated for compensation of the state variables. Therefore, the calculation time becomes prohibitive if multiple switching events occur, posing a limit on the number of GDS transitions that can be handled in a single simulation step [13], [15]. In cases where more than one GDS transition usually happen per subcircuit within a simulation time step, higher accuracy can be obtained by employing oversampling methods that operate at the component level, as will be described in the next subsection.

B. Switch-level GDS Oversampling

Differently from previous method, the Switch-level GDS Oversampling is implemented at component level. This means that, instead of relying on the compensation of the state variables after the GDS transition is identified, it actually restructures the power converter model. For that, instead of purely using the ideal switch concept, the switching transitions of every externally commuted switch are modeled by means of controlled voltage and current sources, whose values are defined taking into account the average value of the GDS over the simulation time step. This average value (duty cycle) is calculated based on the digital input oversampling. Therefore, if the GDS resolution is high enough so that the quantization error can be neglected, it is possible to compensate all GDS transitions within that simulation step. Moreover, since the simulation step period is small in comparison to the switching period, the switching ripple will be preserved [13].

To illustrate that, let us consider an IGBT leg, as shown in Figure 5(a). Figure 5(b) shows the implementation of this IGBT Leg component using the Switch-level GDS Oversampling method. Notice that a pair of diodes is also included to support direction-dependent current flow and natural commutation, as well as to enable discontinuous conduction mode.

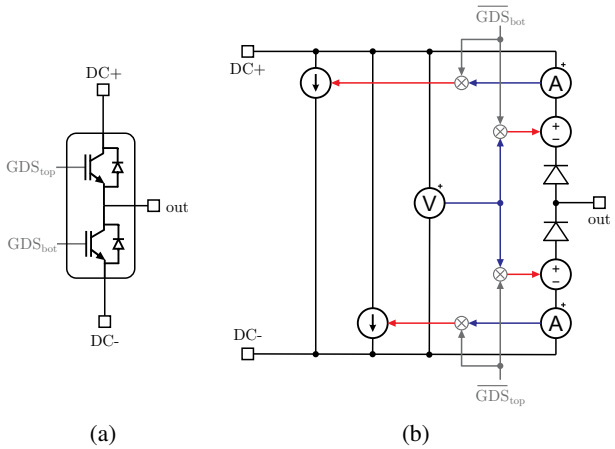

(a) (b)

Fig. 5. IGBT leg: (a) ideal component; (b) implementation based on the Switch-level GDS Oversampling method.

For the IGBT leg shown in Figure 5, the Switch-level GDS Oversampling working principle can be summarized by the following steps:

1. Calculation of the average switching signals over the simulation time step ($\overline{\mathrm{GDS}}_{\mathrm{bot}}$ and $\overline{\mathrm{GDS}}_{\mathrm{top}}$) for every controllable switch. Recall that duty cycles are calculated very precisely thanks to small GDS oversampling period.
2. The converter receives information about duty cycles of the gate drive signals. Together with current and voltage measurements, these information are used to control the current and voltage sources and to define the converter's output, as shown in Figure 5(b).

As mentioned before, this method allows to compensate all GDS transitions within one simulation step, which is an advantage when compared to the Global GDS Oversampling. Nevertheless, due to algorithm complexity, it also includes a delay of one simulation step between GDS inputs and the state outputs. Moreover, since the model has to be restructured including controlled sources and diodes, it is more complex and computationally expensive then the previous approach.

It is important to recall that while a large variety of models works well with Global GDS Oversampling, Switch-level GDS Oversampling method is indicated for those models which rely on high switching frequencies and where more than one GDS transition often happen during one simulation step. A Typical example are the DAB converters. This case study will be presented in the next section, together with a comparison between the two aforementioned oversampling methods.

IV. Case Study: DAB Converter

The DAB converter was proposed in [16] as a high-power-density bidirectional DC/DC topology. By means of soft switching, the converter is capable of reducing switching losses, therefore enabling operation with high switching frequency. The topology of the DAB converter comprises two single-phase full-bridge inverters and a high-frequency transformer, as illustrated in Figure 6. The series inductor L_D is also highlighted in the figure and, in practice, it represents the leakage inductance of the transformer [17].

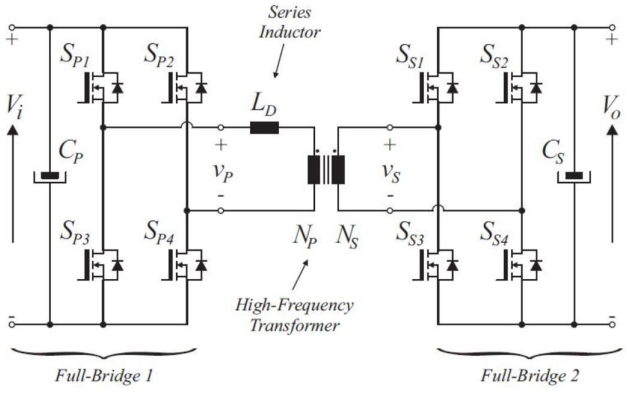

Fig. 6. Topology of the DAB converter [17].

Taking advantage of characteristics such as efficiency, reliability and inherent galvanic isolation, DAB converters have been used in different cutting-edge applications, such as uninterrupted power supplies, microgrids and bidirectional EV chargers. For instance, [18] presents a discrete non-linear controller to regulate the output voltage of a DAB converter operating at 20 kHz, taking into account parametric variations. Suitable results are obtained by means of C-HIL real-time simulations using Typhoon HIL402 device. Regarding EV applications, [6] provides an overview of the advantages of DAB converters for grid-to-vehicle and vehicle-to-grid applications. The system is emulated using Typhoon HIL602 device, and high quality real-time simulation results are provided.

In order to control the DAB converter, the conventional strategy is based on the two-level modulation with phase shift, called single phase shift (SPS). Using this strategy, the power flow can be controlled by changing the phase difference between the carrier signals of the two inverter bridges, while keeping a constant duty cycle. Nevertheless, even with a simple control structure such as SPS, DAB converters operating at high frequencies can be really demanding to simulate in real-time with high precision.

To illustrate that, let us take as a case study the DAB converter with parameters detailed in Table I. Notice that two different switching frequencies (f_{sw}) are considered, in order to compare the simulation performance with the two oversampling methods under different operating conditions.

TABLE I
Case Study: Parameters of the DAB Converter

Parameters	Values	
Maximum power	100 kW	
Input and output voltages	$V_i = 800$ V and $V_o = 400$ V	
Transformer ratio (N_p:N_s)	1 : 1	
Series resistance	$R_D = 100$ mΩ	
Switching frequencies	$f_{sw1} = 50$ kHz	$f_{sw2} = 250$ kHz
Series inductor	$L_{D1} = 8$ μH	$L_{D2} = 1.6$ μH

V. Real-Time Simulation Results

In this section, C-HIL real-time simulation results are presented for the DAB with parameters given in Table I. The converter is emulated on the Typhoon HIL404 device, with a simulation time step of 250 ns and GDS sampling period of 3.5 ns, employing the oversampling methods presented in Section III. Once again, open-loop operation is considered to avoid that controller performance influences the assessment of the simulation accuracy. The SPS modulation is implemented in the DSP TMS320F28379D, from Texas Instruments.

A. Operation with switching frequency of $50\ kHz$

Initially, consider operation of the DAB converter with switching frequency of 50 kHz and a phase shift PS=50^o. For real-time simulation employing the Global GDS Oversampling method, Figure 7 shows the current through the series inductor L_D, as well as the voltages at the primary and secondary of the transformer (V_p and V_s, respectively). Although the

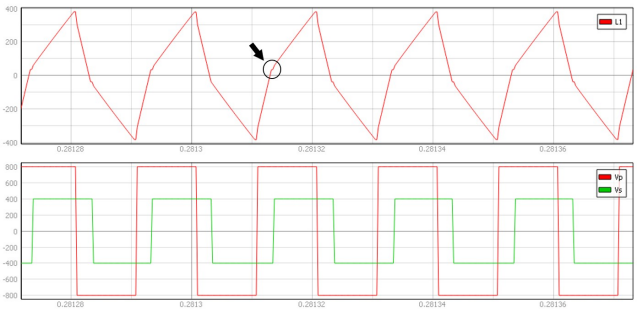

Fig. 7. Operation with $f_{sw} = 50$ kHz and PS $= 50^{o}$ using Global GDS Oversampling method: (top) current through L_D; (bottom) voltages at the primary and secondary of the transformer.

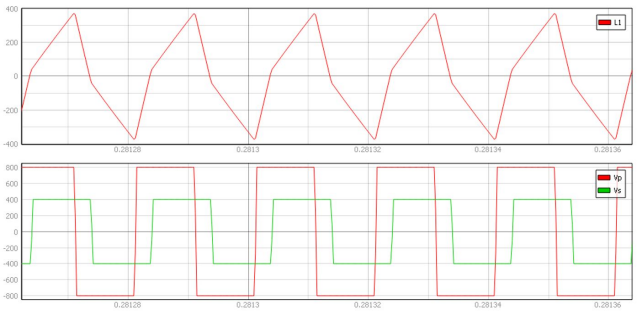

Fig. 8. Operation with $f_{sw} = 50$ kHz and PS $= 50^{o}$ using Switch-level GDS Oversampling method: (top) current through L_D; (bottom) voltages at the primary and secondary of the transformer.

overall results are suitable, it is possible to see that there is an undesired behavior on the current waveforms close to the zero-crossing region, which can be attributed to the multiple GDS transitions and high switching frequency.

On the other hand, Figure 8 shows the waveforms for the same operating conditions, but now obtained with real-time simulation employing the Switch-level GDS Oversampling. One can notice that the undesired behavior pointed out in the previous current waveform is no longer existent, leading to more accurate results. To better illustrate how this affect the overall accuracy of the simulation in different operation points, Figure 9 shows the average output power as function of the phase shift angle employing both oversampling methods. As a reference, the theoretical output power is also plotted [18]. It is possible to verify that both oversampling methods are able to follow the theoretical curve with good precision. Nevertheless, the switch-level GDS oversampling method leads to a slightly better accuracy when compared to the Global oversampling, specially when the phase shift approaches limit values.

B. Operation with 250 kHz

Let us now consider operation of the DAB converter with 250 kHz, while maintaining the phase shift at 50^{o}. For the real-time simulation employing the Global GDS Oversampling method, Figure 10 shows the current and voltages waveforms. Differently from Figure 7, we can notice now a larger imprecision in the current waveform, which is caused by higher

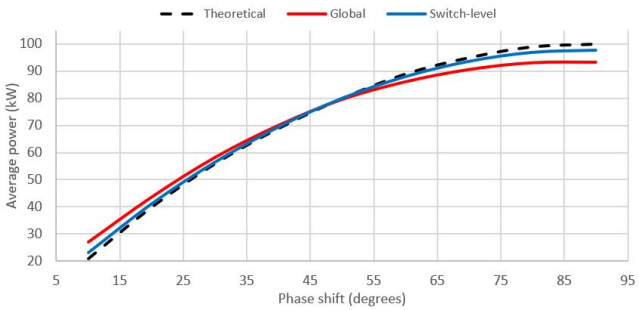

Fig. 9. Average output power as function of the phase shift angle for operation with switching frequency of 50 kHz.

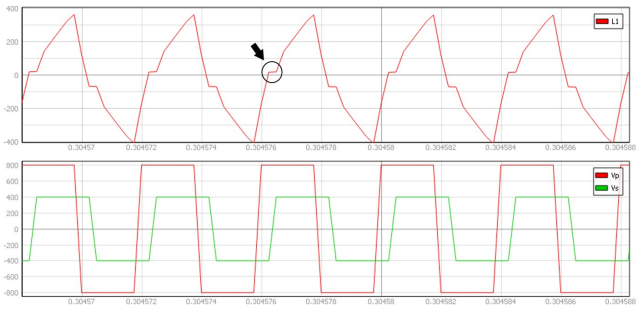

Fig. 10. Operation with $f_{sw} = 250$ kHz and PS $= 50^{o}$ using Global GDS Oversampling method: (top) current through L_D; (bottom) voltages at the primary and secondary of the transformer.

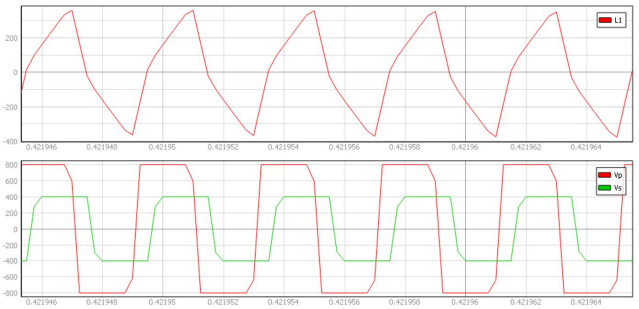

Fig. 11. Operation with $f_{sw} = 250$ kHz and PS $= 50^{o}$ Switch-level GDS Oversampling method: (top) current through L_D; (bottom) voltages at the primary and secondary of the transformer.

GDS sampling errors associated to the significantly higher switching frequency. In opposition, by employing the Switch-level GDS Oversampling method it is possible to properly compensate multiple GDS transitions within a simulation time step, leading to the current waveform shown in Figure 11, where the undesired behavior seen in the previous result was eliminated. The effect of the Switch-level GDS oversampling method can also be seen comparing the voltage waveforms in Figure 10 to the respective ones in Figure 11.

Figure 12 shows the average output power as function of the phase shift angle employing both oversampling methods for operation with 250 kHz. As expected, the Switch-level GDS Oversampling leads to very accurate results. However, differ-

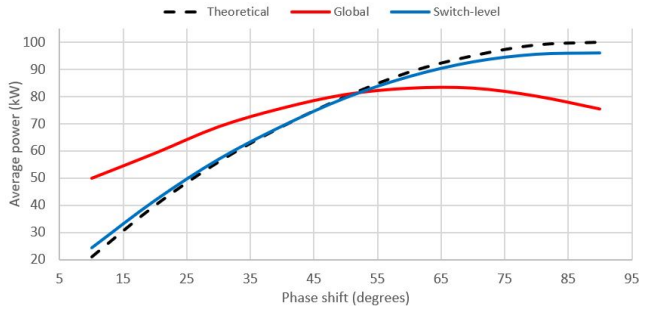

Fig. 12. Average output power as function of the phase shift angle for operation with switching frequency of 250 kHz.

ently from what was concluded for operation with 50 kHz, the Global GDS Oversampling is no longer able to ensure suitable results for the entire range of operation.

Finally, Table II shows a comparison of the computational resource utilization when running without oversampling and also when employing the aforementioned oversampling approaches. As expected, although able to achieve more accurate results, the Switch-level GDS Oversampling method is more complex and computationally expensive, requiring a higher time slot and matrix memory utilization then the Global GDS Oversampling method. It is worth to notice that the utilization values presented in Table II consider that the converter stage is emulated in a single core. Nevertheless, using Typhoon HIL404 device, circuits can be partitioned into up to 4 cores, allowing to reduce hardware utilization and emulate considerably larger systems.

TABLE II
COMPARISON OF THE COMPUTATIONAL RESOURCE UTILIZATION

	None	Global	Switch-Level
Time slot utilization	72.86%	84.29%	98.57%
Matrix memory utilization	34.47%	34.47%	61.94%
Computational latency (simulation steps)	1	2	2

VI. CONCLUSION

This paper presented how enhancements on sampling resolution enabled the use of C-HIL technology to achieve high fidelity real-time simulation results for high switching frequency applications. Firstly, the Global GDS Oversampling method was introduced, and results obtained for a boost converter confirmed that this approach can mitigate the insufficient sampling resolution of the driving signal, improving the accuracy of the simulation for PE applications. Then, the Switch-level GDS Oversampling method was presented, detailing how it is able to compensate multiple switching events within a simulation time step. A DAB converter was taken as case study to illustrate the performance of both oversampling methods, confirming that the presented approaches allow to significantly extend the range of switching frequencies that can be handled with high accuracy by C-HIL real-time simulation.

REFERENCES

[1] M. Liserre, T. Sauter, and J. Y. Hung, "Future Energy Systems: Integrating Renewable Energy Sources into the Smart Power Grid Through Industrial Electronics," *IEEE Industrial Electronics Magazine*, vol. 4, no. 1, pp. 18–37, 2010.

[2] C. R. D. Osório, G. G. Koch, H. Pinheiro, R. C. L. F. Oliveira, and V. F. Montagner, "Robust Current Control of Grid-Tied Inverters Affected by LCL Filter Soft-Saturation," *IEEE Transactions on Industrial Electronics*, vol. 67, no. 8, pp. 6550–6561, 2020.

[3] K. Knezović, S. Martinenas, P. B. Andersen, A. Zecchino, and M. Marinelli, "Enhancing the Role of Electric Vehicles in the Power Grid: Field Validation of Multiple Ancillary Services," *IEEE Transactions on Transportation Electrification*, vol. 3, no. 1, pp. 201–209, 2017.

[4] V. Dinavahi, M. Reza Iravani, and R. Bonert, "Real-Time Digital Simulation of Power Electronic Apparatus Interfaced with Digital Controllers," *IEEE Transactions on Power Delivery*, vol. 16, no. 4, pp. 775–781, 2001.

[5] M. S. Vekić, S. U. Grabić, D. P. Majstorović, I. L. Čelanović, N. L. Čelanović, and V. A. Katić, "Ultralow Latency HIL Platform for Rapid Development of Complex Power Electronics Systems," *IEEE Transactions on Power Electronics*, vol. 27, no. 11, pp. 4436–4444, 2012.

[6] A. Khan, F. Jarraya, A. Gastli, L. Ben-Brahim, R. Hamila, and K. Rajashekara, "Dual Active Full Bridge Implementation on Typhoon HIL for G2V and V2G Applications," in *2017 IEEE Vehicle Power and Propulsion Conference (VPPC)*, 2017, pp. 1–6.

[7] A. Genic, P. Gartner, M. Almeida, and D. Zuber, "Hardware In the Loop Testing of Shipboard Power System's Management, Control and Protection," in *2017 IEEE Vehicle Power and Propulsion Conference (VPPC)*, 2017, pp. 1–6.

[8] R. Salcedo, E. Corbett, C. Smith, E. Limpaecher, R. Rekha, J. Nowocin, G. Lauss, E. Fonkwe, M. Almeida, P. Gartner, S. Manson, B. Nayak, I. Celanovic, C. Dufour, M. Faruque, K. Schoder, R. Brandl, P. Kotsampopoulos, T. H. Ha, A. Davoudi, A. Dehkordi, and K. Strunz, "Banshee Distribution Network Benchmark and Prototyping Platform for Hardware-in-the-Loop Integration of Microgrid and Device Controllers," *The Journal of Engineering*, vol. 2019, pp. 5365–5373(8), August 2019.

[9] A. Genić, P. Gartner, D. Medjo, and M. Dinić, "Multi-Layer Hardware-in-the-Loop Testbed for Microgrids," in *2016 International Conference on Smart Systems and Technologies (SST)*, 2016, pp. 95–102.

[10] D. Majstorovic, I. Celanovic, N. D. Teslic, N. Celanovic, and V. A. Katic, "Ultralow-Latency Hardware-in-the-Loop Platform for Rapid Validation of Power Electronics Designs," *IEEE Transactions on Industrial Electronics*, vol. 58, no. 10, pp. 4708–4716, 2011.

[11] N. Pallo, T. Foulkes, T. Modeer, E. Fonkwe, P. Gartner, and R. C. Pilawa-Podgurski, "Hardware-in-the-Loop Co-Design Testbed for Flying Capacitor Multilevel Converters," in *2017 IEEE Power and Energy Conference at Illinois (PECI)*, 2017, pp. 1–8.

[12] Typhoon HIL, "Documentation – GDS Oversampling." [Online]. Available: typhoon-hil.com/documentation/typhoon-hil-software-manual/concepts/gds_oversampling.html

[13] K. Lian and P. Lehn, "Real-Time Simulation of Voltage Source Converters Based on Time Average Method," *IEEE Transactions on Power Systems*, vol. 20, no. 1, pp. 110–118, 2005.

[14] Typhoon HIL, "4th Generation HIL. Built for the most advanced motor drive and automotive applications," 2020. [Online]. Available: info.typhoon-hil.com/hil404-technicalpaper

[15] M. Faruque, V. Dinavahi, and W. Xu, "Algorithms for the Accounting of Multiple Switching Events in Digital Simulation of Power-Electronic Systems," *IEEE Transactions on Power Delivery*, vol. 20, no. 2, pp. 1157–1167, 2005.

[16] R. De Doncker, D. Divan, and M. Kheraluwala, "A Three-Phase Soft-Switched High-Power-Density DC/DC Converter for High-Power Applications," *IEEE Transactions on Industry Applications*, vol. 27, no. 1, pp. 63–73, 1991.

[17] A. L. Kirsten, R. F. Coelho, T. A. Pereira, F. Jung, and D. Jelic, "Typhoon HIL Application Note – Dual Active Bridge with Pulse Width Modulation based on Signal Processing." [Online]. Available: typhoon-hil.com/documentation/typhoon-hil-application-notes/References/dab_with_sp_based_pwm.html?hl=dab

[18] E. L. Santos da Silva, A. Luís Kirsten, and D. J. Pagano, "Discrete SPS Control of a DAB converter using partial Feedback Linearization," in *2019 IEEE 15th Brazilian Power Electronics Conference and 5th IEEE Southern Power Electronics Conference (COBEP/SPEC)*, 2019, pp. 1–6.